Supplementary Information for: "Probing spin-dependent charge transport on the single nanometer scale"

Patrick Härtl,[1,*] Markus Leisegang,[1] Jens Kügel,[1] and Matthias Bode[1,2]

[1] *Physikalisches Institut, Experimentelle Physik II, Universität Würzburg, Am Hubland, 97074 Würzburg, Germany*

[2] *Wilhelm Conrad Röntgen-Center for Complex Material Systems (RCCM), Universität Würzburg, Am Hubland, 97074 Würzburg, Germany*

(Dated: February 3, 2023)

I. ROTATIONAL STATES OF HPC ON BIAG$_2$

HPc adsorbed on $BiAg_2$ exhibits, next to the four tautomeric states, three rotational states. As shown in the topographic images of Fig. S1, three rotational states of molecules coexist, which are rotated by 120° towards each other and which will be labeled Rot A, Rot B, and Rot C hereafter. In each case the molecular arms are rotated by 45° from the substrates high-symmetry axes. A detailed study of the rotational behavior and the influence of the individual states on remote excitation has been reported in a recent study by us [S1]. In this work we have shown that two distinct axes with different electron yields for tautomerization exist, resulting in a significant influence of the rotational state on the remote excitation. Moreover, the MONA measurements have revealed that these three states Rot A, Rot B, and Rot C are equally populated, indicating their equivalence.

Within a MONA measurement, each data point includes several thousand single injection and detection events. Based on the statistical nature and the rather low probability for a rotation, however, which is by a factor of 30 lower as compared to a tautomerization [S1], the absolute number of states Rot A, Rot B, and Rot C within an individual data set deviates. To account for this statistical variation and to correct the influence of an unequal state population, we weighted the experimentally determined tautomeric electron yield of all three rotational states by a factor of 1/3 which results in a realistic expectation value.

In the following three sections, we will discuss the data presented in the main text with regard to the three rotational states. All data were recorded in remanence while the tip was pre-treated in an external out-of-plane oriented magnetic field of ±2 T. The

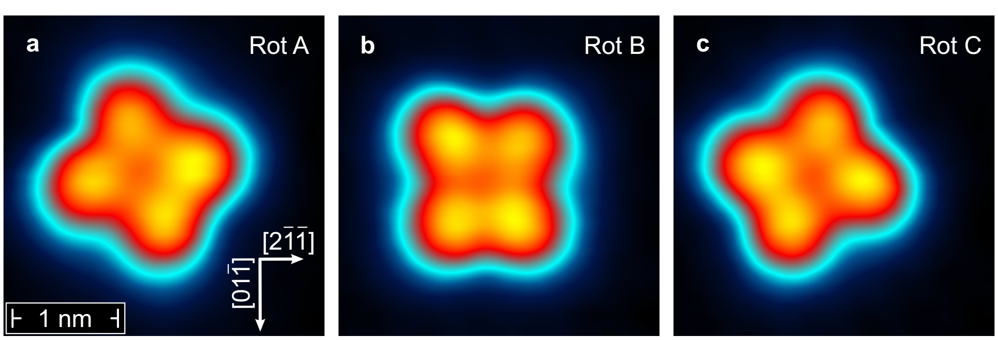

FIG. S1. **The three rotational states of HPC on BiAg$_2$.** STM images of the states **a** Rot A, **b** Rot B, and **c** Rot C, which are rotated by 120° against each other. Scan parameters: $U_{\text{scan}} = 100 \ldots 200\,\text{meV}$, $I_{\text{scan}} = 30 \ldots 40\,\text{pA}$.

asymmetry A_α of the electron yields η at a given angle α can be calculated as $A_\alpha = \left(\eta_\alpha^{+2\,\mathrm{T}} - \eta_\alpha^{-2\,\mathrm{T}}\right) / \left(\eta_\alpha^{+2\,\mathrm{T}} + \eta_\alpha^{-2\,\mathrm{T}}\right)$.

II. NON-MAGNETIC TIP

Figure S2 shows spin-averaged MONA data recorded with a non-magnetic tungsten tip for all three rotations individually (a-c) as well as the total electron yield in (d) (non-weighted). MONA parameters are $E_{\mathrm{exc}} = 650\,\mathrm{meV}$, $t_{\mathrm{exc}} = 2.0\,\mathrm{s}$, $I_{\mathrm{exc}} = 1.0\,\mathrm{nA}$. The corresponding weighted data are shown in Fig. 2(a) of the main text. In all four plots, within the error bar the electron yield shows no correlation with the magnetic history, i.e., whether the data were recorded after a field sweep to positive or negative field.

However, a significant deviation between different angles can be found within one rotational state as well as for the same angle between the three rotational states. While the $0° - 180°$ axis shows a low electron yield for Rot A and Rot C, a high yield is observed along

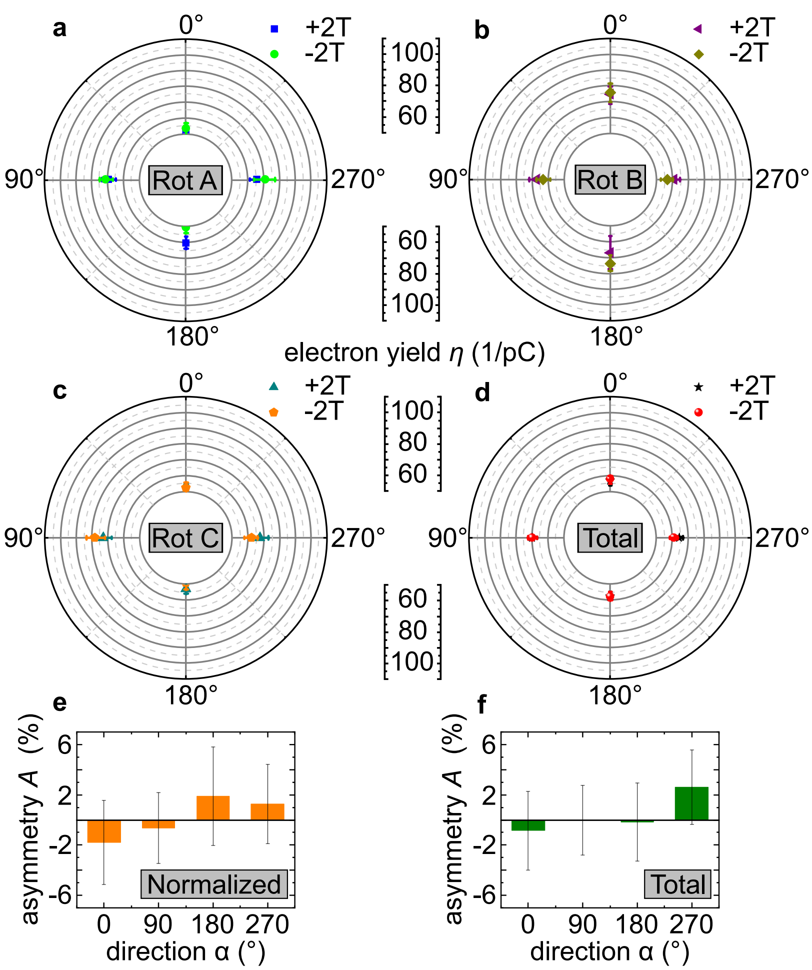

FIG. S2. **MONA data for an unpolarized W-tip.** In **a**, **b**, and **c**, the data for the spin-averaged measurement set [main text Fig. 2(a)] are plotted individually for each molecular rotation Rot A, Rot B and Rot C, respectively. All data have been measured in remanence (0 T) after exposing the tip to an external magnetic field of ±2 T. **d**, The non-weighted total electron yield, neglecting the influence of the rotations. **e**, Weighted asymmetries of the data presented in Fig. 2(a) in the main text. **f**, Asymmetries of the non-weighted total electron yield presented in **d**.

this axis for Rot B. This behavior inverts for the $90° - 270°$ axis. Now Rot A and Rot C have a high and Rot B has a low electron yield. As reported in detail in our recent publication, these observations can be explained by the combination of the four fold symmetric molecular cage with the six fold symmetric substrate [S1]. Since two rotational states (Rot A and Rot B) exhibit the same behavior, they dominate the total electron yield (non-weighted) shown in Fig. S2(d) where the $90° - 270°$ axis has a higher yield as compared to the $0° - 180°$. For comparison, the calculated asymmetry A for the weighted and not-weighted averaged electron yield are presented in Fig. S2(e) and (d), respectively. In both cases, within the error bars no significant asymmetry can be found.

III. MAGNETIC TIP

Figure S3 shows spin-polarized MONA data recorded with a magnetically Gd-coated tip for the three rotational states (a-c), as well as the total electron yield in (d) (non-weighted). The corresponding weighted data are shown in Fig. 2(b) of the main text. MONA parameters are $E_{\mathrm{exc}} = 650\,\mathrm{meV}$, $t_{\mathrm{exc}} = 2.0\,\mathrm{s}$, $I_{\mathrm{exc}} = 1.0\,\mathrm{nA}$ at a distance of $d = 4.0\,\mathrm{nm}$ from the molecule under four different angles. All four plots show a qualitative similar behavior. The two-fold symmetry of the electron yield with an inversion for Rot B is equivalent to what has been discussed for the unpolarized measurements. However, a significant deviation between the field sweeps can be observed. While the electron yields for both field sweeps ($\pm 2\,\mathrm{T}$) are comparable along the $0° - 180°$ direction, a significant difference can be observed along the $90° - 270°$ axis for all three rotations as well as for the total sum. The calculated asymmetries A for the weighted electron yields of the main text (Fig. 2(b)) as well as for the non-weighted total yield of Fig. S3 (d) are plotted in Fig. S3(e) and (f), respectively. Both plots reveal a similar behavior of A, while the absolute values slightly differ between the weighted and non-weighted electron yield η. Since all three rotations exhibit a significant asymmetry along the $90° - 270°$ axis, we can exclude a direct influence by the rotations.

Additional SP-MONA data, acquired with a macroscopically different magnetically Gd-coated tip, are presented in Figure S4. MONA parameters are $E_{\mathrm{exc}} = 650\,\mathrm{meV}$, $t_{\mathrm{exc}} = 2.0\,\mathrm{s}$, $I_{\mathrm{exc}} = 1.5\,\mathrm{nA}$ at a distance of $d = 4.5\,\mathrm{nm}$ from the molecule. These measurements provide a higher angular resolution with eight angles which are again plotted separately for all three rotations as well as the non-weighted total yield. The corresponding weighted data are

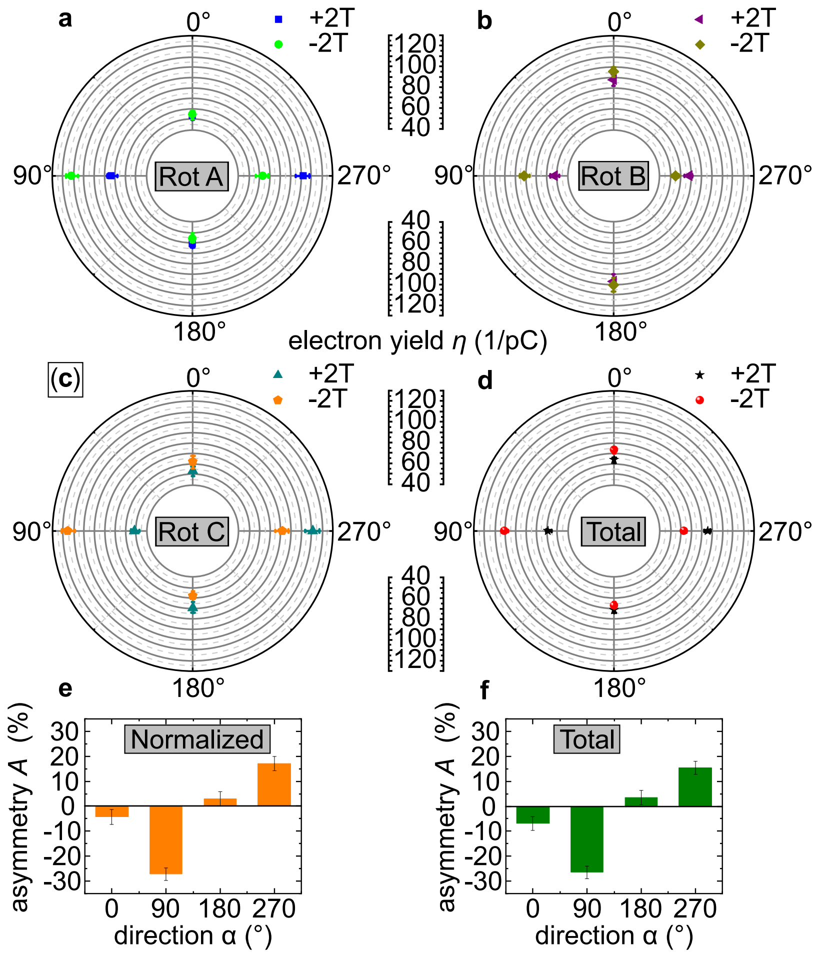

FIG. S3. **MONA data measured with a magnetically coated Gd tip.** In **a**, **b** and **c** the data for the spin-polarized measurement set [main text Fig. 2(b)] are plotted individually for each molecular rotation Rot A, Rot B and Rot C, respectively. All data have been measured in remanence (0 T) after exposing the tip to an external magnetic field of ±2 T. **d**, The non-weighted total electron yield, neglecting the influence of the rotations. **e**, Weighted asymmetries for the data presented in Fig. 2(b) in the main text. **f**, Asymmetries for the non-weighted total electron yield presented in **d**.

shown in the main text Fig. 2(c). The dashed lines serve only as a guide to the eye. Due to the higher resolution, a two-fold mirror symmetric electron yield can be observed for all three rotations. The plots show a rotation of roughly 120° towards each other, which is in line with the molecular rotations on the surface. However, the axis of high and low asymmetry A are always pointing along the $45° - 225°$ and $135° - 315°$ axes, respectively. These axes can also be identified in the non-weighted total electron yield in Fig. S4(d). The resulting asymmetry is shown in Figure S4(e), where a cosine-like behavior can be fitted to the graph in accordance to the weighted data shown in the main text Fig. 2(c) and (d).

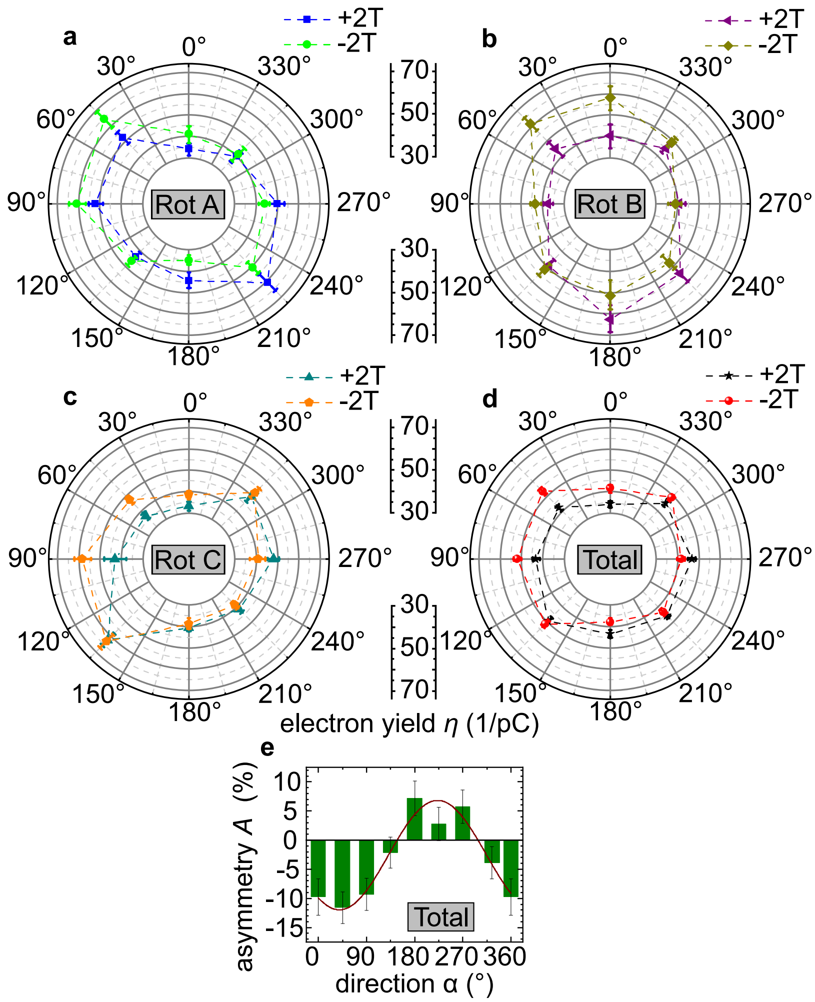

FIG. S4. **High angular resolution spin-polarized MONA measurement.** In **a**, **b** and **c** the data for the spin-polarized measurement set [main text Fig. 2(c)] are plotted individually for each molecular rotation Rot A, Rot B and Rot C, respectively. All data have been measured in remanence (0 T) after exposing the tip to an external magnetic field of ±2 T. **d**, The non-weighted total electron yield, neglecting the influence of the rotations. **e**, Asymmetries for the non-weighted total electron yield presented in **d** with a cosine fit (brown line). The dashed lines in **a**, **b**, **c**, and **d** serve as a guide to the eye only.

IV. MONA ON A CLUSTER

In this measurement, a Gd-cluster has been placed in the 90° direction as a magnetic impurity. Charge carriers were injected by a Gd-coated tip. MONA parameters are $E_{\mathrm{exc}} = 650\,\mathrm{meV}$, $t_{\mathrm{exc}} = 2.5\,\mathrm{s}$, and $I_{\mathrm{exc}} = 2.0\,\mathrm{nA}$ at a distance of $d = 6.5\,\mathrm{nm}$ from the molecule. The data are presented equivalently to the spin-averaged and spin-polarized data sets of Figs. S2 and S3, respectively. In the three plots of Fig. S5(a)-(c) we document the results obtained for all molecular rotation listed above. The averaged data of Fig. S5(d) clearly reveal the influence of the Gd cluster under 90°. The asymmetry shown in Fig. S5(e) clearly deviates from a cosine-like behavior, highlighting the strong influence of the cluster. The weighted data of this experimental run are shown in the main text Fig. 3(b) and (d).

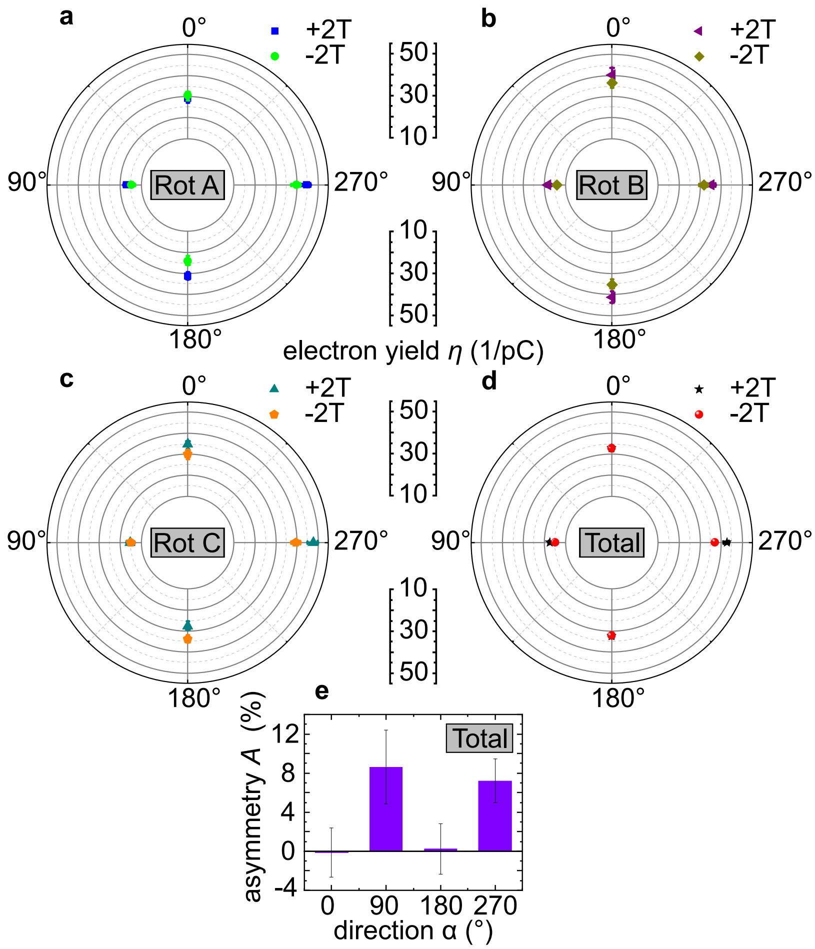

FIG. S5. **SP-MONA data with a Gd-cluster.** In **a**, **b** and **c** the data for the spin-polarized measurement set [main text Fig. 3(b)] are plotted individually for each molecular rotation Rot A, Rot B and Rot C, respectively. All data have been measured in remanence (0 T) after exposing the tip to an external magnetic field of ±2 T. **d**, The non-weighted total electron yield, neglecting the influence of the rotations. **e**, Asymmetries for the non-weighted total electron yield presented in **d**.

An equivalent representation is given for a HPc without any defect nearby, acting as reference system for the measurements with a cluster. This setup has been probed on the very same surface with the same Gd-coated tip in a distance of around 30 nm to the setup with cluster. The data in Figure S6 show an equivalent cosine-like behavior (see asymmetry in Figure S6(e)) as discussed for the SP-MONA data in Figure S3 as well as the same signature originating from the molecular rotations.

V. PRE-CHARACTERIZATION OF THE MAGNETIC TIP ON GD/W(110)

In this section, the preparation and characterization of a magnetically Gd-coated tip is described. W tips are electro-chemically etched in a NaOH solution, carefully rinsed with distilled water, transferred into the ultra-high vacuum (UHV) system via a load lock, and then cleaned in several high-temperature flashes from potential contamination by e-beam heating.

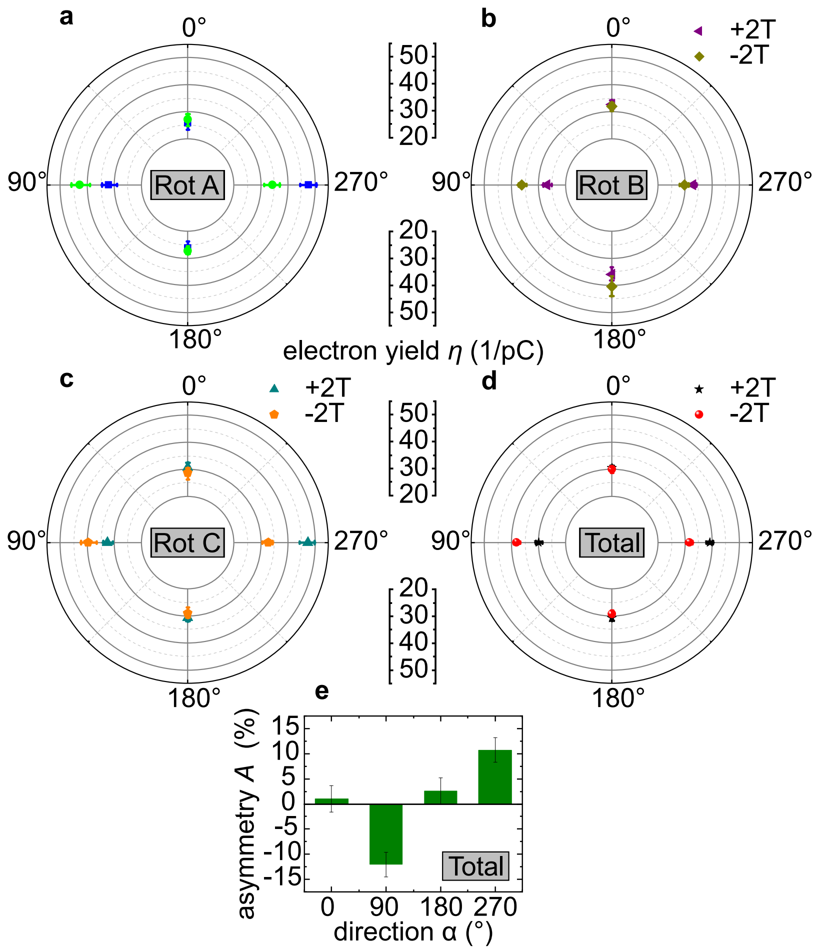

FIG. S6. **Reference SP-MONA data without a Gd-cluster.** In **a**, **b** and **c** the data for the spin-polarized measurement set [main text Fig. 3(c)] are plotted individually for each molecular rotation Rot A, Rot B and Rot C, respectively. All data have been measured in remanence (0 T) after exposing the tip to an external magnetic field of ±2 T. **d**, The non-weighted total electron yield, neglecting the influence of the rotations. **e**, Asymmetries for the non-weighted total electron yield presented in **d**.

To magnetize these initially non-magnetic tips, we utilize Gd(0001)/W(110) films which were investigated by us in a recent SP-STM study [S2]. Fig S7(a) shows the topography of a 200 AL Gd film grown on a W(110) substrate. This film was deposited at a deposition rate of (19.8 ± 3.7) AL per minute onto the substrate held at room temperature. Subsequent annealing for five minutes at $T_{\mathrm{anneal}} \geq 900\,\mathrm{K}$ results in a very flat and highly ordered surface, see Ref. S2 for details.

The transfer of magnetic material (Gd) from this sample to the tip is achieved by dipping the tip a few nanometers into the Gd film or by gentle pulsing $U_{\mathrm{bias}} > 4\,\mathrm{V}$. To our experience both procedures may result in the attachment of a Gd cluster to the tip. To verify that the transfer resulted in a magnetically sensitive tip, we measured differential conductance $\mathrm{d}I/\mathrm{d}U$ maps at $E - E_{\mathrm{F}} = E_{\mathrm{exc}} = 650\,\mathrm{meV}$. Only if the tip is indeed magnetically sensitive, a zig-zag pattern with two distinct contrast levels like the one shown in Fig. S7(c) appears, which is characteristic for the domain structure of Gd films in this thickness range [S2]. At the points marked in the bright (red star) and the dark area (black star), $\mathrm{d}I/\mathrm{d}U$ point spectra were

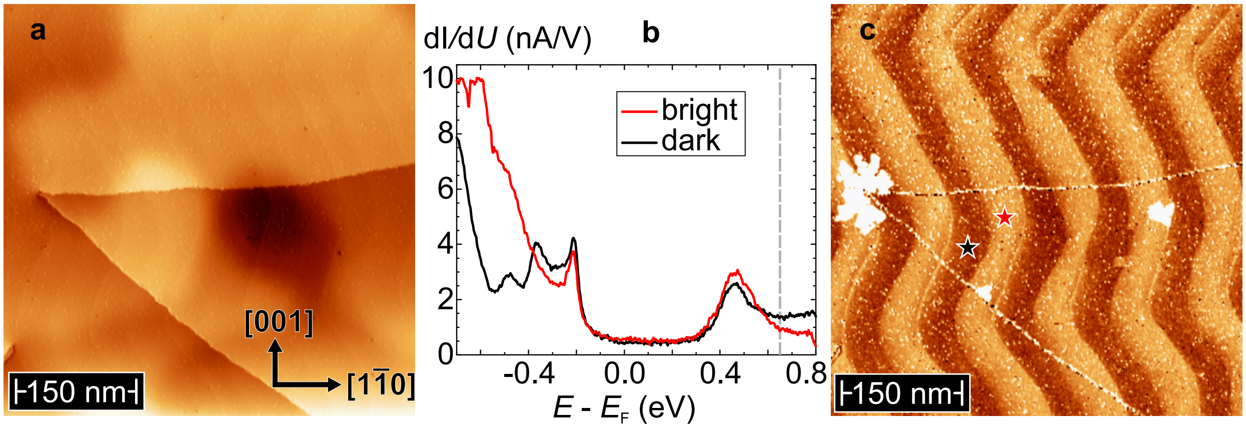

FIG. S7. **Tip pre-characterization on Gd/W(110).** **a**, Overview scan of a 200 AL Gd film epitaxially grown on a W(110) substrate. **b**, $\mathrm{d}I/\mathrm{d}U$ point spectra taken at the positions marked by a red/black star in (**c**), revealing a tip polarization at $E - E_\mathrm{F} = E_\mathrm{exc} = 650\,\mathrm{meV}$ (grey dashed line). **c**, Magnetically sensitive $\mathrm{d}I/\mathrm{d}U$ map of the film presented in (**a**). A zig-zag like domain pattern along the W[001] direction can be identified, comparable to the data already published by Härtl *et al.* [S2]. Scan parameters: $U_\mathrm{bias} = 650\,\mathrm{mV}$, $I_\mathrm{set} = 1\,\mathrm{nA}$.

taken at a frequency of $f_\mathrm{mod} = 5.309\,\mathrm{kHz}$ (well above the cutoff frequency of the feedback loop) and with a modulation of $U_\mathrm{bias} = 10\,\mathrm{mV}$. These spectra are plotted in Fig. S7(b). The significant difference between theses spectra evidences its suitability for spin-polarized experiments. Most important for the measurements presented in this contribution is the fact that we find a significant polarization at $E - E_\mathrm{F} = E_\mathrm{exc} = 650\,\mathrm{meV}$, marked by a grey dashed line in Fig. S7(b).

VI. POST-CHARACTERIZATION OF THE MAGNETIC TIP ON FE/W(110) ML-ISLANDS

After successful SP-MONA measurements on $BiAg_2$, we verified the tip polarization by post-characterization on Fe/W(110) monolayer islands. This is an ideal test system, since the islands exhibit a well-defined in-plane magnetization along the $[\bar{1}\bar{1}0]$ direction of the W(110) substrate [S3]. This direction is aligned with the $0° - 180°$ axis in our SP-MONA experiments.

Fe was deposited onto the clean W(110) substrate from a rod with a diameter of 2 mm via an electron beam evaporator at a flux of 10 nA for 30 s deposition, leading to a coverage of $\approx 0.24\,\mathrm{AL}$. During growth the substrate is held at a temperature $T_\mathrm{sample} \approx 400\,\mathrm{K}$. The

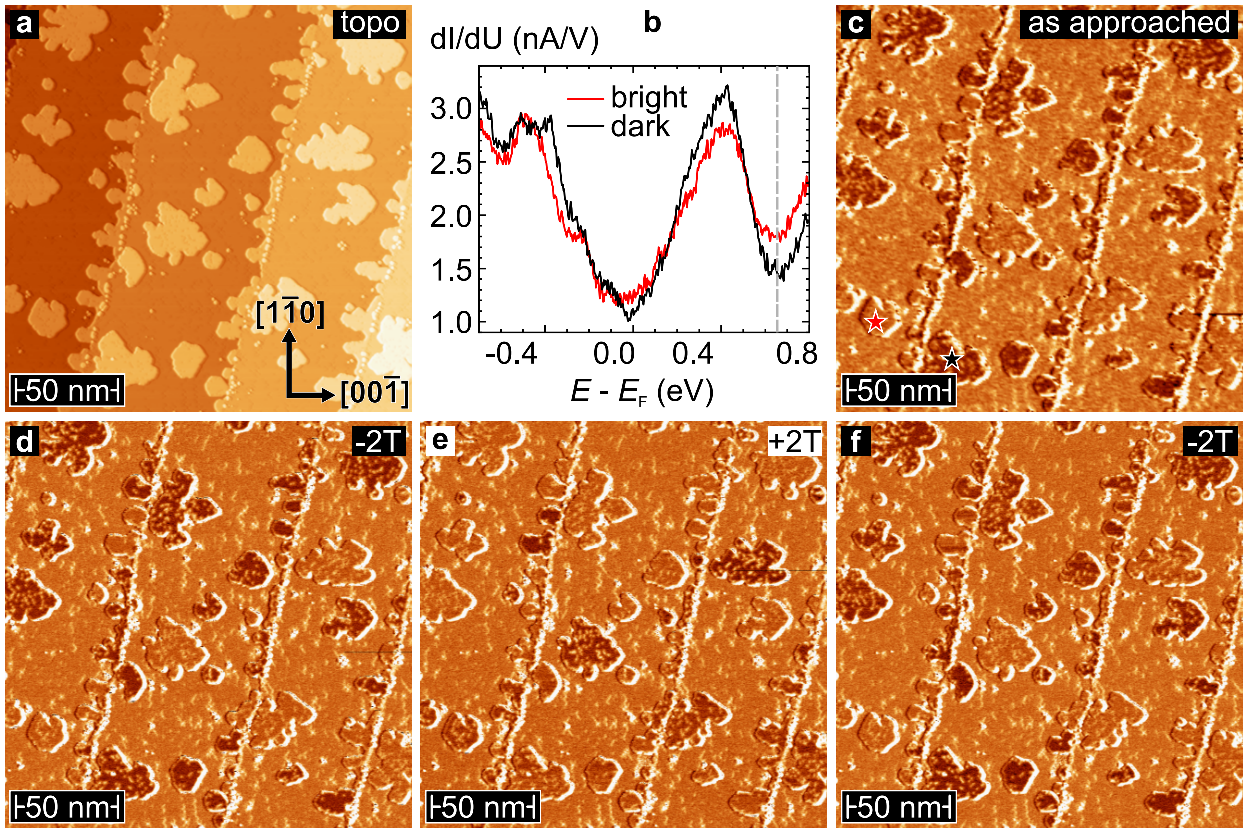

FIG. S8. **Post-characterization of the magnetic tip on Fe/W(110) ML-islands.** **a**, Topography of Fe monolayer islands on W(110) at a Fe coverage of ≈ 0.24 AL. **b** $\mathrm{d}I/\mathrm{d}U$ point spectra measured on the Fe islands marked with a red/black star in (**c**), revealing a significant tip polarization at $E - E_\mathrm{F} = 650\,\mathrm{meV}$ (see grey hatched line) after the SP-MONA measurements. **c**, $\mathrm{d}I/\mathrm{d}U$ map directly recorded after the SP-MONA measurement presented in Fig. 3 of the main text. The islands show two different contrast levels, indicating a significant in-plane polarization component of the magnetic STM tip. **d**, $\mathrm{d}I/\mathrm{d}U$ map of the region shown in (**c**) after tip-treatment at -2 T, measured in remanence. **e**, $\mathrm{d}I/\mathrm{d}U$ map after a field ramp to +2 T, measured in remanence. **f**, $\mathrm{d}I/\mathrm{d}U$ map after a field ramp back to -2 T, where the islands again inverted their contrast. STM parameters: $U_\mathrm{bias} = 650\,\mathrm{mV}$, $I_\mathrm{set} = 1\,\mathrm{nA}$.

resulting islands on the stepped substrate can be seen in the overview scan of Fig.S8(a).

To verify that the tip is sensitive to the in-plane component of the magnetization at the energy used for our SP-MONA experiments, i.e., $E - E_\mathrm{F} = E_\mathrm{exc} = 650\,\mathrm{meV}$, we measured differential conductance $\mathrm{d}I/\mathrm{d}U$ maps at exactly this energy. The corresponding image in Fig. S8(c) shows islands with two different contrast levels, indicating a significant in-plane polarization of the tip after the SP-MONA measurements. At the positions marked with the red (bright island) star and the black (dark island) star, $\mathrm{d}I/\mathrm{d}U$ point spectra are taken. The resulting spectra are plotted in Fig. S8(b), confirming a significant spin polarization at

$E - E_\mathrm{F} = E_\mathrm{exc} = 650\,\mathrm{meV}$ (grey dashed line).

Subsequently, we verified that the in-plane component along the $[\bar{1}\bar{1}0]$ direction of the W(110) substrate can indeed be reversed successfully by the application of an external magnetic field. We exposed the tip to fields of $-2\,\mathrm{T}$, $+2\,\mathrm{T}$ and back to $-2\,\mathrm{T}$. After each field ramp the magnetic state of the tip was investigated at remanence ($0\,\mathrm{T}$). For this purpose, we measured $\mathrm{d}I/\mathrm{d}U$ images taken at the same sample location. As can be seen by comparing the data sets presented in Fig. S8(d)-(f), the contrast levels of the islands inverted after each field sweep, thereby verifying the fact that the magnetization of the spin-sensitive tip used for the SP-MONA measurements presented in Fig. 3 can be (i) reversed with the available external magnetic fields, (ii) exhibits a significant spin polarization at the energy used in SP-MONA experiments ($E - E_\mathrm{F} = E_\mathrm{exc} = 650\,\mathrm{meV}$), and (iii) that the tip magnetization exhibits a significant in-plane component, i.e., in the plane where a spin-polarized transport of spin–momentum-locked Rashba states is expected.

---

* corresponding author: patrick.haertl@physik.uni-wuerzburg.de

[S1] M. Leisegang, M. Böhme, D. Maiberger, P. Härtl, J. Kügel, and M. Bode, “Electron-Induced Switching Processes of Phthalocyanine Molecules on (3×3) Bi/Ag(111)R30°: Tautomerization Accompanied by Rotation,” The Journal of Physical Chemistry C **127**, 592 (2023).

[S2] P. Härtl, M. Leisegang, and M. Bode, “Magnetic domain structure of epitaxial Gd films grown on W(110),” Phys. Rev. B **105**, 174431 (2022).

[S3] S. Krause, L. Berbil-Bautista, G. Herzog, M. Bode, and R. Wiesendanger, “Current-Induced Magnetization Switching with a Spin-Polarized Scanning Tunneling Microscope,” Science **317**, 1537–1540 (2007).